

2017 IEEE International Conference on Advanced Intelligent Mechatronics (AIM)  
Sheraton Arabella Park Hotel, Munich, Germany, July 3-7, 2017

## Bandwidth Extension of Hybrid-Reluctance-Force-based Tip/Tilt System by Reduction of Eddy Currents

Ernst Csencsics, Johannes Schlarp, and Georg Schitter

**Abstract**—This paper investigates the influence of eddy currents on the dynamic behavior of a novel hybrid-reluctance-force actuator for tip/tilt systems. The effects of eddy currents on the mechatronic system dynamics are identified and modeled by a first order system approximation. Their influence on the achievable performance of a closed loop controlled system is studied by investigating two configurations of the ferromagnetic actuator yoke. An initial solid steel configuration of the yoke is compared to a layered yoke structure with isolated steel sheets, with the aim to improve the system bandwidth, which is limited by the eddy currents. Robust PID feedback controllers are designed for controlling the mover position of both system configurations, resulting in comparable phase margins. Experiments demonstrate that the closed loop bandwidth of the prototype setup can be increased from 370 Hz to 1 kHz by changing the yoke structure, which equals a bandwidth improvement by a factor of 2.8.

### I. INTRODUCTION

Fast steering mirrors (FSMs) are opto-mechatronic tip/tilt systems that are used in various applications. The applications can be subdivided into pointing and scanning tasks, with tracking of objects [1] and stabilization of optical systems [2] being typical pointing applications. The variety of applications for scanning systems includes optical free space communication [3], scanning optical lithography [4], material processing [5] and laser scanners [6]. Depending on the application requirements tip/tilt system are typically actuated by voice coil (range up to 35 mrad with a limited bandwidth of several 100 Hz) [6] or piezo actuators (bandwidth up to several kHz but range of single milliradians) [7]. This clearly requires a tradeoff in the range-bandwidth performance, as it is difficult to realize large bandwidth and large range simultaneously.

This tradeoff could be relaxed by employing reluctance force actuators [8]. Due to the higher force density as compared to voice coil actuators [9] and larger working ranges as compared to piezos, they have the potential to enable system designs with extended range-bandwidth products. Even though hardly used in the past, due to several challenges, such as non-linear force-current relation or the ability to exert only pulling forces [9], [10], several implementations of reluctance force actuator designs for linear motion in fast servo tools [11] and valve engines [12], as well as for active vibration isolation systems [8] have been reported recently. Reluctance actuators have also already been employed for first FSM system designs, achieving a large closed-loop

bandwidth of 2 kHz for the case of internal capacitive sensors and 10 kHz with a fast external optical sensor, but only limited range of  $\pm 3.5$  mrad [3]. Another design study presents a more compact version, which, however, also sticks to the initial structure with four distinct actuators placed around the mover, limiting their potential for highly compact and integrated FSM designs [13].

To extend the angular range and to enable more compact system designs, a novel hybrid reluctance tip/tilt actuator has been developed [14]. The performance goals for the first prototype of this new design, formulated in Table I, result from a review of specifications of available tip/tilt systems and consideration of requirements of target applications in scanning optical metrology systems.

TABLE I  
HYBRID ACTUATOR TARGETED PERFORMANCE GOALS.

Parameter	Performance goal
Angular range	$\pm 3^\circ$
Bandwidth	1 kHz
Angular acceleration	$5e3 \text{ rad/s}^2$
Mover diameter	56 mm

Particularly for small and compact FSM systems it would be beneficial to manufacture the ferromagnetic system parts out of a solid material. From other applications such as transformers [15], magnetic bearings [16] and actuators [17] eddy currents, defusing in the ferromagnetic components, are, however, known to be sources of performance limiting effects, especially towards high frequencies. Usually these effects are reduced by assembling the ferromagnetic parts from isolated layers of sheet material. For the new hybrid reluctance actuator prototype it is, however, not clear to which extent eddy currents affect the achievable system performance and which core structure is required to achieve the targeted performance goals.

This paper investigates the influence of eddy currents in the ferromagnetic yoke of the novel hybrid-reluctance actuator on the achievable closed-loop performance of a tip/tilt system prototype. For this purpose two system configurations, one with a solid and one with a layered yoke, are realized, identified and modeled. In Section II the working principle of the hybrid-reluctance actuator is explained. The prototype system setup is presented in Section III, followed by the system identification and modeling of the dynamics in Section IV. In Section V feedback controllers are designed for both system configurations and in Section VI the closed

The authors are with the Christian Doppler Laboratory for Precision Engineering for Automated In-Line Metrology at the Automation and Control Institute (ACIN), Vienna University of Technology, 1040 Vienna, Austria. Corresponding author: [csencsics@acin.tuwien.ac.at](mailto:csencsics@acin.tuwien.ac.at).

loop performance is evaluated. Section VII concludes the paper.

## II. ACTUATOR WORKING PRINCIPLE

The tip/tilt system is based on a novel 2 degree of freedom (DoF) hybrid reluctance actuator design, which is a modification of a linear motion hybrid actuator [8], [18]. Fig. 1 shows a cross-section view of the hybrid actuator along one actuator axis and provides an overview of the system components. The actuator components with the yoke (green),

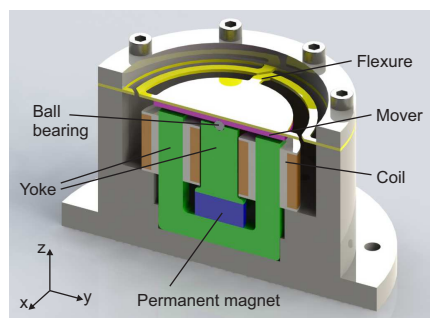


Fig. 1. CAD cross section view of the hybrid actuator along one system axis. The permanent magnet (blue), the yoke parts (green) and the actuator coils (orange) are shown. The mover (magenta) rests on a ball bearing on the center yoke part and is suspended by a mechanical flexure (yellow).

the permanent magnet (blue), the actuator coils (orange) and the mover (magenta) are observable. Further the flexure (yellow) suspending the mover is shown. The second actuator axis is identical and is arranged perpendicularly to the first axis. The yoke parts of both axes are connected beneath the magnet.

Fig. 2 depicts the working principle of the hybrid actuator. The permanent magnet in the center of the actuator generates a DC biasing flux (red line) which passes through the center yoke part and the non-working air gap and returns via the working air gaps and the outer yoke parts. When the coil current is zero and the mover is in the middle position the magnetic flux is equally distributed over the working air gaps and there is no net torque on the mover. Due to the high reluctance of permanent magnet to outer magnetic fields, the magnetic flux generated by a coil current (coils connected in series) passes only through the mover and the outer yoke parts. The two fluxes are superimposed in the working air gaps resulting in an increased and weakened flux in the right and left air gap, respectively, resulting in a clockwise net torque on the mover. Reverting the current direction results in a counterclockwise torque. The actuation principle itself is inherently unstable due to negative stiffness introduced by the reluctance forces.

The suspension system comprises an aluminum flexure and an additional ball bearing between the center yoke part and the mover. The flexure is compliant along the two actuated rotational DoFs and constrains the translational DoFs along the  $x$ - and  $y$ -axis and the rotational DoF around the  $z$ -axis. The ball bearing supports the preloading forces

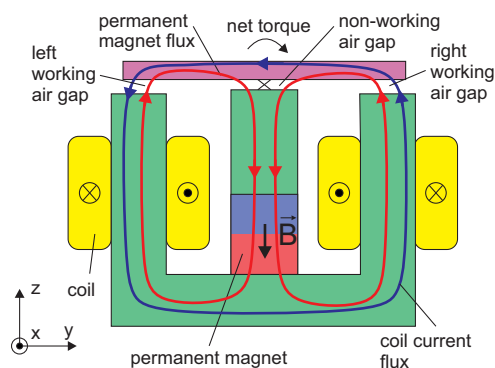


Fig. 2. Hybrid reluctance force actuation principle. The biasing flux (red) from the permanent magnet is divided over both outer yoke parts. The steering flux (blue) of the coil current strengthens and weakens the biasing flux in the right and left air gap respectively. This results in a clockwise torque on the ferromagnetic mover (magenta).

due to the permanent magnet and constrains the translational DoF along the  $z$ -axis. The flexure is directly bonded to the mover (see Fig. 1), such that the moving part has a minimal inertia. It is designed to compensate for the negative stiffness of the actuation principle, resulting in an open loop stable system and enabling an open loop system identification.

The FSM prototype has a range of  $\pm 3^\circ$  in tip and tilt, a mover diameter of 56 mm and an outer diameter of 100 mm. The force is almost linear with respect to current, with a small remaining position dependency of the force/current ratio. A more detailed description and analysis of the actuator properties can be found in [14].

## III. PROTOTYPE SYSTEM

### A. Actuator Yoke Configuration

The actuator prototype system is designed for high performance scanning applications, which typically require feedback motion control to achieve the required precision. They further typically require several degrees of angular range and rather high scan speeds. Additional benefits of the actuation concept are that no additional components are attached to the mover (increasing the inertia), as it is the case for moving coil or magnet designs of voice coil actuators, and the potential for a high level of integration in small and compact systems. To maintain feasibility of such compact systems, it is desirable that the yoke components can be manufactured out of solid ferromagnetic material. Literature, however, shows that with solid yokes additional dynamics due to eddy currents affect the system dynamics [17] by introducing an additional phase lag (see Section IV and Fig. 4). To reduce these effects layered yoke structures composed of several isolated material sheets, as known from transformers [15] and other actuators [3], can be used to reduce the formation of eddy currents and their bandwidth limiting effects.

As it is not clear how severely eddy currents affect the dynamics and limit the achievable performance of the new

hybrid actuator concept, two different yoke configurations are investigated (see Fig.3).

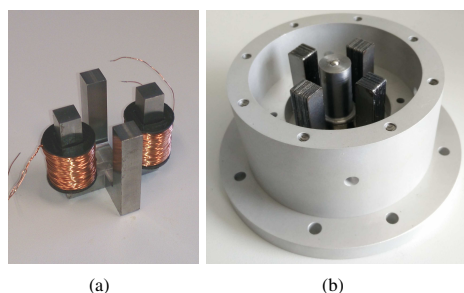


Fig. 3. Hybrid actuator yoke configurations. (a) shows the solid yoke with coils mounted for one system axis. (b) depicts the layered yoke placed in the aluminum base structure. Further the center yoke part with the biasing magnet on the bottom and the ball bearing on top is shown.

First a solid 10x10 mm steel yoke is tested, which is then replaced by a layered yoke configuration made of 0.5 mm steel sheets (EN 10025 S 235 JR) with isolation coating on both sides. Thinner sheets of material may also be possible but as the material fill factor (ratio steel/coating) for given yoke dimensions decreases with the sheet thickness, there is always a tradeoff between eddy current reduction and saturation flux required. With 0.5 mm sheets and a coating of 0.03 mm on both sides, a material fill factor of 89% can be achieved for the given yoke dimensions. Using for example 0.1 mm sheets instead and the same coating, the fill factor drops to 62%. This reduces the maximum magnetic flux that can pass through the yoke without saturation, which is directly proportional to the motor constant of the actuator [14], [18]. The yoke dimensions are chosen with the aim to avoid yoke saturation (given results of FEM simulations) and maintain a material fill factor of about 90%.

According to the description of the working principle from the previous section the actuator yoke part can be divided into DC and high frequency flux paths. The center yoke part is only traversed by the DC biasing flux of the permanent magnet and can thus be made of a solid ferromagnetic material. The outer yoke parts are traversed by the time varying steering flux. The mover, even though also traversed by the time varying steering flux, is made of solid steel due to structural stability and manufacturing reasons.

### B. Setup Electronics

A custom made current amplifier (Amplifier type MP38CL, Apex Microtechnology, Tucson, AZ, USA) is used to drive the coils of each actuator axis. The actuator has relatively high inductance of about 1 mH due to its ferromagnetic yoke. This high inductance is a challenge for the power amplifiers, as they need to provide high current and voltage at higher driving frequencies, so that a small number of coil turns with 70 turns per coil is used. The prototype actuator has thus a smaller motor constant in order to not limiting the system performance by the amplifier supply voltage. As the amplifier also has to dissipate the

majority of the required power (only a small percentage is dissipated through actuator losses) the supply voltage is set to 30 V and an appropriate heatsink is attached, to stay within the thermal limits. PI current controllers with a bandwidth of 30 kHz are used to control the amplifiers (see Fig. 5) and are implemented in the FPGA of a dSpace-platform (Type: DS1202, dSPACE GmbH, Germany). To measure the rotational position of the mover in 2DoF differential eddy current displacement sensor systems (eddyNCDT DT3702-U1-A-C3, Micro-Epsilon GmbH, Germany) are used. They are mounted to the aluminum base, are positioned above the mover and measure the angles directly via a linear approximation for small angles.

## IV. IDENTIFICATION OF EXPERIMENTAL SYSTEM

For identification of the system dynamics of both prototype setups a system analyzer (3562A, Hewlett-Packard, Palo Alto, CA, USA) is used. The inputs of the current amplifiers and the signals of the position sensors are considered as the system inputs and outputs, respectively.

The frequency response data of a single axis of the systems with solid yoke (blue) and layered yoke (red) are both shown in Fig. 4. The suspension modes of the systems

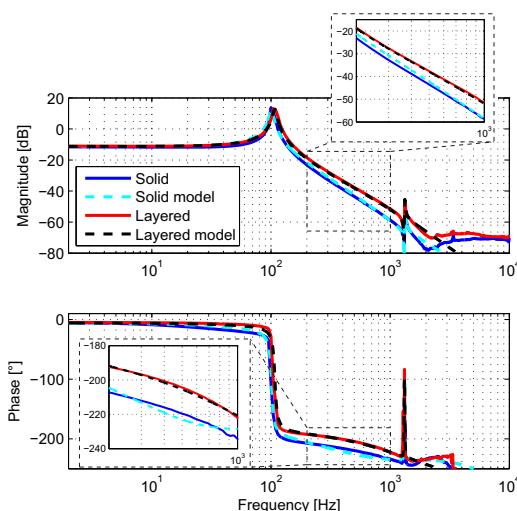


Fig. 4. Frequency response of a single system axis with solid yoke (solid blue) and layered yoke (solid red) at 500 mA drive current amplitude. Additionally the system models for both cases (solid yoke - dashed cyan, layered yoke - dashed black) are shown. The layered yoke shows less phase lag and a less steep magnitude slope beyond 100 Hz.

lie at 101 Hz and 108 Hz for the solid and layered yoke system, respectively. The zero-pole-combination at around 1.35 kHz is the first structural mode of the designed flexure (predicted by FEM simulations) and similar for both system configurations. The small variation of the system dynamics around the suspension mode are due to assembly tolerances. The structural mode is well above the targeted bandwidth and not a limiting factor from controls perspective. Both systems

have a common phase lag due to sensor dynamics (10 kHz bandwidth) and sampling delay ( $f_s=45$  kHz).

The system with the solid yoke configuration shows a -50 dB/dec magnitude slope above the suspension mode instead of the expected -40 dB/dec slope of a typical mass-spring system. Further it shows a significant phase lag towards higher frequencies which is already  $-219.5^\circ$  at 500 Hz. Both effects are clearly limiting the bandwidth of position feedback controls. Considering a typical PID feedback controller with a maximum phase lead of about  $50^\circ$  [18], a unity gain crossover of the loop gain at 500 Hz would result in a phase margin (PM) of only  $10.5^\circ$ . These effects are due to eddy current in the solid yoke parts, which can be concluded from looking at the frequency response of the system with the layered yoke configuration and comparing it with the solid yoke system. The layered yoke system has a magnitude slope of approximately -45 dB/dec and shows less phase lag of about  $-204.5^\circ$  at 500 Hz. This means that by changing the yoke configuration of the system a significant phase difference of about  $15^\circ$  can be gained in a frequency range between 200 Hz and 900 Hz (see zoomed image in Fig. 4).

To model the dynamic effects of the eddy currents in the system, first the relation

$$\Phi(s) = \frac{\mu A_p N}{l_{mc}} \cdot \frac{\tanh(\alpha b)}{\alpha b} \cdot i_c(s), \quad (1)$$

between magnetic flux  $\Phi$  and coil current  $i_c$  in a reluctance actuator can be established, which results from diffusion equations for flux density or magnetic field strength [16], [17], [19]. The relation holds for a ferromagnetic yoke with  $a \gg b$ , where in this case  $a$  and  $b$  are the width and thickness of the yoke layers, respectively. In (1)  $A_p$  represents the cross section area of the yoke,  $N$  the number of coil turns and  $l_{mc}$  the effective length of the magnetic circuit. The parameter  $\alpha$  is defined by  $\alpha^2 = s\sigma\mu$ , with  $\mu$  and  $\sigma$  being the permeability and conductivity of the yoke material, respectively. According to (1) and the parameter  $\alpha$  the transfer function (TF)  $\Phi(s)/i_c(s)$  is a transcendental function of  $s$ . Using a series expansion for the fraction depending on  $\alpha$  [20] and approximating all but the dominating first term of the series expansion, the approximation

$$\Phi(s) = \frac{\mu A_p N}{l_{mc}} \cdot 1.044 \cdot \frac{1 + sT_e \cdot 0.224}{1 + sT_e} \cdot i_c(s), \quad (2)$$

for (1), with  $T_e = 4\sigma\mu b^2/\pi^2$  can be obtained.

The dynamics of both system configurations (with sensor dynamics  $S(s)$  and sampling delay  $T$ ) without eddy current effects can be modeled by

$$G(s) = K \cdot \frac{\omega_0^2}{s^2 + 2\omega_0\zeta_0 s + \omega_0^2} \cdot \frac{s^2 + 2\omega_1\zeta_1 s + \omega_1^2}{s^2 + 2\omega_2\zeta_2 s + \omega_2^2} \cdot S(s) \cdot e^{-sT}, \quad (3)$$

with  $S(s)$  a first order lowpass (10 kHz bandwidth), a sampling delay  $T = 1/f_s$  and parameters according to Table II.

As the constant gain of (2) is already included in  $G(s)$ , only the additional lag-lead term needs to be taken into

account for the modeling. The resulting entire plant model of the layered yoke system is thus found by

$$P(s) = G(s) \cdot \frac{1 + sT_e \cdot 0.224}{1 + sT_e}. \quad (4)$$

With yoke parameters according to Table III the parameter  $T_e = 115 \mu s$  can be calculated for the layered yoke system.

TABLE II  
MODEL COEFFICIENTS FOR BOTH SYSTEM CONFIGURATIONS.

Yoke	K	Index	$\omega_{Index}$ [rad/s]	$\zeta_{Index}$
Solid	1.135e5	0	635	0.031
		1	8.23e3	0.003
		2	8.39e3	0.004
Layered	1.29e5	0	679	0.031
		1	8.23e3	0.003
		2	8.36e3	0.004

The modeling of the eddy current dynamics, including the approximation and the derivation of  $T_e$ , is no more valid for the solid yoke system, as  $a = b$ . However, a fitted lag-lead term with a pole at 398 Hz and a zero at 2.1 kHz can still be used to model the dynamics due to the eddy currents. The resulting system models for the solid (dashed cyan) and layered yoke system (dashed black) are also depicted in Fig. 4. It can be seen that the resulting models are in a good agreement with the measured responses and can be used to describe the system dynamics in the frequency range of interest up to about 1 kHz.

TABLE III  
PARAMETERS OF FERROMAGNETIC YOKE.

Parameter	Description	Value
$a$	Yoke width	10 mm
$b_s$	Solid yoke thickness	10 mm
$b_l$	Layered yoke thickness	0.5 mm
$\mu_r$	Relative permeability	2500
$\sigma$	Conductivity	2.9e6 S/m

## V. CONTROLLER DESIGN AND IMPLEMENTATION

For feedback control of the hybrid actuator tip/tilt system the cascaded control structure shown in Fig. 5 is employed for each system axis. The tip/tilt actuator is denoted by  $P(s)$ ,

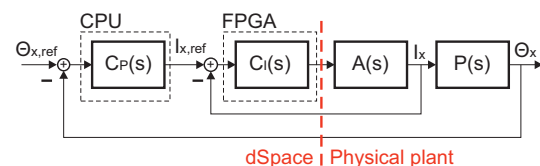


Fig. 5. Control structure applied to each axis of the hybrid actuator. The current controller  $C_I(s)$  (inner loop) controls the output current of the amplifier  $A(s)$ . The position controller  $C_P(s)$  controls the angular position  $\Theta_x$  of the mover in one dimension.

driven by the power amplifier  $A(s)$ .  $C_I(s)$  and  $C_P(s)$  are the

current and position controller, respectively. Measurement of the crosstalk magnitudes (data not shown) between the system axes revealed that at low frequencies the crosstalk is more than 21 dB smaller than the response of the scanning axes, which denotes sufficient decoupling and justifies the use of single-input-single-output (SISO) controllers. To ensure sufficient robustness of the feedback system a PM of at least  $30^\circ$  is targeted.

#### A. Position Controller Design

For controlling the position of the mover of the solid yoke system a PID controller is designed [18]. Due to the phase lag of the system the crossover frequency is limited to 200 Hz in order to maintain the targeted PM. The P-gain shifts the magnitude slope in order to place the intersection between mass- and 0 dB line to the targeted crossover frequency. The D-gain is designed such that the D-action shows the maximum phase lead at the crossover frequency. A realization term stops the D-action by placing a pole at 660 Hz to limit the control effort at higher frequencies. The I-gain increases the loop gain at low frequencies and reduces the steady state error of the closed loop system. As the low crossover frequency requires only a comparably small P-gain the structural mode is not critical for the closed loop stability as the loop gain stays well below the 0 dB line at this frequency. The resulting controller for the solid yoke system has the form

$$C_{P,s}(s) = K \cdot \frac{s^2 + 2\omega_z \zeta_z s + \omega_z^2}{(s + \omega_{p1}) \cdot (s + \omega_{p2})}, \quad (5)$$

with parameters according to Table IV.

Due to the reduced phase lag of the system with the layered yoke configuration, the PID controller for position control of the mover can be designed for a crossover frequency of 500 Hz. The P-gain can be tuned higher due to the higher crossover frequency. Also the D-action is shifted to higher frequencies as compared to  $C_{P,s}(s)$ . To ensure stability of the system when closing the loop, the PID controller is extended by a notch filter at 1330 Hz that compensates the structural mode of the flexure, to ensure a sufficient gain margin. The resulting controller for the layered yoke system is given by

$$C_{P,l}(s) = K \cdot \frac{\left( \prod_{i=1}^2 s^2 + 2\omega_{z_i} \zeta_{z_i} s + \omega_{z_i}^2 \right)}{\left( s^2 + 2\omega_{p1} \zeta_{p1} s + \omega_{p1}^2 \right) \cdot \left( \prod_{i=2}^3 s + \omega_{p_i} \right)}, \quad (6)$$

with parameters according to Table IV.

#### B. Controller Implementation

For implementation of both controllers in the processor of the dSpace system, they are discretized for a sampling frequency of  $f_s=45$  kHz by using Pole-Zero-Matching. The frequency responses of the implemented position controllers  $C_{P,s}(s)$  and  $C_{P,l}(s)$  (data not shown) show a clearly reduced P-gain of  $C_{P,s}(s)$  and that the D-gain together with the maximum phase lead of the controller  $C_{P,l}(s)$  is centered

around the higher crossover frequency. The notch filter in  $C_{P,l}(s)$  has only a marginal influence on the phase lead of the controller at crossover.

TABLE IV  
COEFFICIENTS OF DESIGNED POSITION CONTROLLERS.

Controller	K	Index	$\omega_{Index}$ [rad/s]	$\zeta_{Index}$
$C_{P,s}$	51.9	$z$	219	0.89
		$p_1$	0.628	-
		$p_2$	4.15e3	-
$C_{P,l}$	224	$z_1$	552	0.89
		$z_2$	8.38e3	0.006
		$p_1$	8.38e3	0.03
		$p_2$	6.28	-
		$p_3$	1.04e4	-

## VI. EXPERIMENTAL RESULTS

The resulting system performance is evaluated and compared in terms of PM and achieved closed-loop bandwidth.

The open loop frequency responses of the two system configurations with the related controllers are shown in Fig. 6. The solid yoke system shows significantly smaller

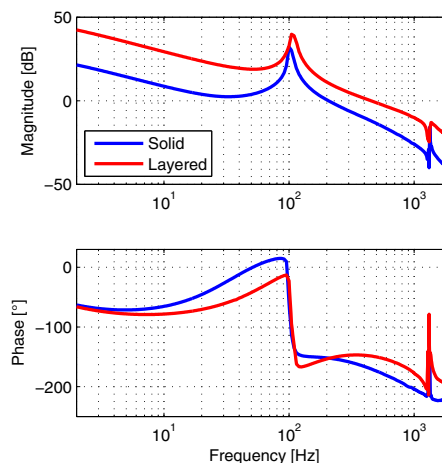


Fig. 6. Open loop frequency responses of the solid yoke (blue) and layered yoke (red) system configuration. The crossover frequencies are at 206 Hz and 452 Hz for the system with solid and layered yoke, respectively.

gain at low frequencies and even approaches the 0 dB line around 30 Hz, denoting a low loop gain and reduced tracking performance in this frequency range. The structural mode of the flexure is well below the 0 dB line and is not compromising the stability when closing the loop. The loop gain has the crossover frequency at 206 Hz and a gain margin (GM) of 16 dB. The PM is  $28^\circ$  and thus slightly below the targeted PM of  $30^\circ$ . The layered yoke system has a significantly higher loop gain at low frequencies due to its higher crossover frequency. The suppression of the resonance of the structural mode by the notch filter can be clearly seen, such that the GM is not reduced. The crossover frequency is at 452 Hz, yielding a GM of 11.3 dB, that is slightly

smaller than in the case of the solid yoke system. The PM is  $31^\circ$ , fulfilling the initial design target. The comparison confirms that for the same PM in case of the solid yoke system the achievable crossover frequency is more than a factor of two lower compared to the layered yoke system, due to the increased phase lag.

Fig. 7 shows the measured complementary sensitivity functions of both system configurations with the corresponding controllers. The solid yoke system has a bandwidth of

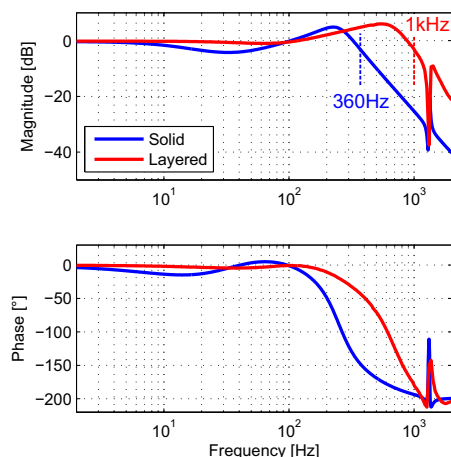


Fig. 7. Complementary sensitivity functions of the solid (blue) and layered yoke (red) system configuration. The -3 dB system bandwidth of the layered yoke system is with 1 kHz significantly larger.

360 Hz and shows a gain peaking of 4.7 dB at 220 Hz. Due to the small loop gain between 10 Hz and 50 Hz the magnitude drops below unity gain in this frequency range. The layered yoke system shows a gain peaking of 6 dB at 550 Hz and has a bandwidth of 1 kHz, which is a factor of 2.8 higher as compared to the solid yoke system.

In summary, the eddy currents at dynamic operation of the FSM system get reduced, resulting in an almost 3 times higher achievable closed-loop bandwidth of the novel hybrid-reluctance-force actuator based tip/tilt system.

## VII. CONCLUSION

In this paper the dynamics of a novel hybrid-reluctance-force actuator for tip/tilt systems are studied, revealing that the eddy currents induced in the yoke at dynamic operation limit the achievable closed loop bandwidth. The eddy current effects are identified, modeled and their influence on the achievable system performance is investigated. To overcome the identified bandwidth limiting phase lag, the initial solid configuration of the yoke is replaced by a layered ferromagnetic yoke structure with isolated material sheets. For controlling the position of the mover in 2DoF, decentralized controllers are designed and tested for both system configurations. It is demonstrated that the bandwidth of the prototype system can be increased by a factor of 2.8 from 370 Hz to 1 kHz by changing the yoke configuration.

For future systems the optimization of the layer thickness for given actuator dimensions may be an important aspect.

## ACKNOWLEDGMENT

The financial support by the Austrian Federal Ministry of Science, Research and Economy and the National Foundation for Research, Technology and Development, as well as MICRO-EPSILON MESSTECHNIK GmbH & Co. KG and ATENSOR Engineering and Technology Systems GmbH is gratefully acknowledged.

## REFERENCES

- [1] M. Guelman, A. Kogan, A. Livne, M. Orenstein, and H. Michalik, "Acquisition and pointing control for inter-satellite laser communications," *IEEE Transactions on Aerospace and Electronic Systems*, vol. 40, no. 4, 2004.
- [2] S. Xiang, P. Wang, S. Chen, X. Wu, D. Xiao, and X. Zheng, "The research of a novel single mirror 2d laser scanner," *Proc. of SPIE*, vol. 7382, 2009.
- [3] D. J. Kluk, M. T. Boulet, and D. L. Trumper, "A high-bandwidth, high-precision, two-axis steering mirror with moving iron actuator," *Mechatronics*, vol. 22, no. 3, 2012.
- [4] Q. Zhou, P. Ben-Tzvi, D. Fan, and A. A. Goldenberg, "Design of fast and steering mirror and systems for precision and laser beams and steering," *IEEE International Workshop on Robotic and Sensors Environments, Ottawa, CAN*, 2008.
- [5] L. R. Hedding and R. A. Lewis, "Fast steering mirror design and performance for stabilization and single axis scanning," *SPIE Vol. 1304 Acquisition, Tracking and Pointing IV*, 1990.
- [6] M. Hafez, T. Sidler, R. Salathe, G. Jansen, and J. Compter, "Design and simulations and experimental and investigations of a compact single mirror tip/tilt laser scanner," *Mechatronics*, vol. 10, 2000.
- [7] F. M. Tapos, D. J. Edinger, T. R. Hilby, M. S. Ni, B. C. Holmes, and D. M. Stubbs, "High bandwidth fast steering mirror," *Optics and Photonics 2005*, 2005.
- [8] D. Laro, R. Boshuisen, J. Dams, and J. van Eijk, "Linear hybrid actuator for active force cancellation," *International Symposium on Linear Drives for Industry Applications*, vol. 8, 2011.
- [9] N. H. Vrijns, J. W. Jansen, and E. A. Lomonova, "Comparison of linear voice coil and reluctance actuators for high-precision applications," *Power Electronics and Motion Control Conference*, 2010.
- [10] A. van Lievenooogen, A. Toma, and U. Ummethala, "Challenges in the application of hybrid reluctance actuators in scanning positioning stages in vacuum with nanometer accuracy and mgauss magnetic stray field," *American Control Conference*, 2013.
- [11] D. Wu, X. Xie, and S. Zhou, "Design of a normal stress electromagnetic fast linear actuator," *IEEE Transactions on Magnetics*, vol. 46, no. 4, 2010.
- [12] J. Kim and J. Chang, "A new electromagnetic linear actuator for quick latching," *IEEE Transactions on Magnetics*, vol. 43, no. 4, 2007.
- [13] Y. Long, C. Wang, X. Dai, X. Wei, and S. Wang, "Modeling and analysis of a novel two-axis rotary electromagnetic actuator for fast steering mirror," *Journal of Magnetics*, vol. 19, no. 2, 2014.
- [14] E. Csencsics, J. Schlarp, and G. Schitter, "High performance hybrid-reluctance-force-based tip/tilt system: Design, control and evaluation," *IEEE Transactions on Mechatronics*, 2017, submitted.
- [15] N. Locci and C. Muscas, "Hysteresis and eddy currents compensation in current transformers," *IEEE Transactions on Power Delivery*, vol. 16, no. 2, 2001.
- [16] L. Zhou and L. Li, "Modeling and identification of a solid-core active magnetic bearing including eddy currents," *IEEE/ASME Transactions on Mechatronics*, vol. 21, no. 6, 2016.
- [17] J. J. Feeley, "A simple dynamic model for eddy currents in a magnetic actuator," *IEEE Transactions on Magnetics*, vol. 32, no. 2, 1996.
- [18] R. Munnig Schmidt, G. Schitter, A. Rankers, and J. van Eijk, *The Design of High Performance Mechatronics*. 2nd Revised Edition, Delft University Press, 2014.
- [19] R. B. Zmood, D. K. Anand, and J. A. Kirk, "The influence of eddy currents on magnetic actuator performance," *IEEE Proceedings*, vol. 75, 1987.
- [20] I. S. Gradshteyn and I. M. Ryzhik, *Table of Integrals, Series and Products*. Academic Press, Orlando FL, 1980.